



# High-Sensitivity Detection of Dichlorvos Using a Multi-Walled Carbon Nanotubes-Gold Nanoparticles/Glassy Carbon Electrode Impedimetric Electrochemical Sensor

Khaisa Avchukir,<sup>1</sup> Yrysgul Bakytkarim,<sup>2,\*</sup> Zhazira Mukatayeva,<sup>2</sup> Yerbol Tileuberdi,<sup>2</sup> Nurgul Shadin,<sup>2</sup> Dilyara Yenbekova<sup>1</sup> and Gulmira Rakhymbay<sup>1</sup>

## Abstract

In this study, we report the fabrication of a novel impedimetric electrochemical sensor for the sensitive and reliable detection of the organophosphorus pesticide Dichlorvos (DDVP). The sensor is based on a glassy carbon electrode (GCE) modified with multi-walled carbon nanotubes (MWCNTs) and gold nanoparticles (AuNPs). MWCNTs provide a large surface area, high conductivity, and mechanical stability, while AuNPs enhance electron transfer and adsorption capability. The synergistic combination of these nanomaterials significantly improves the electrode's sensitivity and selectivity. The detection mechanism is based on the inhibition of interfacial electron transfer resulting from the strong interaction between DDVP and the modified electrode surface. This interaction produces measurable impedance changes, allowing indirect quantification of DDVP. The sensor achieved a low detection limit of 18.8 nM and a wide linear range of 0.36 - 1.8  $\mu$ M ( $R^2=0.99$ ), demonstrating excellent reproducibility and reliability. The developed sensor is label-free, cost-effective, and easy to fabricate, making it suitable for large-scale monitoring. Owing to its simplicity and high performance, this system holds great potential for environmental water analysis, agricultural product testing, and food safety assessment, offering an efficient tool for pesticide monitoring and public health protection.

**Keywords:** Dichlorvos; Indirect detection; Impedimetric electrochemical sensor; Modified electrode; Nanocomposites.

Received: 09 September 2025; Revised: 24 October 2025; Accepted: 12 November 2025

Article Type: Research article.

## 1. Introduction

Organophosphorus (OP) pesticides are a group of highly toxic chemical compounds extensively applied in agriculture due to their rapid degradation in the environment and strong insecticidal activity.<sup>[1]</sup> Their potent neurotoxic effects make them highly effective in protecting crops from a wide range of pests, which has led to their continuous global usage. Among them, Dichlorvos (DDVP; 2,2-dichlorovinyl dimethyl phosphate) is one of the most widely used OP pesticides. Structurally, DDVP is an organophosphate compound applied in the food industry, household pest control, and agricultural practices to combat domestic insects.<sup>[2]</sup> The insecticidal mechanism of DDVP is attributed to its inhibition of acetylcholinesterase (AChE), a key enzyme in the nervous

system responsible for the hydrolysis of the neurotransmitter acetylcholine. The inhibition of AChE results in abnormal accumulation of acetylcholine in synaptic clefts, which causes persistent nerve stimulation, muscular paralysis, and eventually death of the pest.<sup>[3]</sup> In practical applications, DDVP is widely used to control pests such as cockroaches, aphids, mosquitoes, caterpillars, and mushroom flies.<sup>[4]</sup> Despite its effectiveness, DDVP is associated with significant health risks to humans. Scientific studies have reported that exposure to DDVP can lead to adverse symptoms including cyanosis, muscular paralysis, ataxia, seizures, headaches, chest tightness, dyspnea, visual disturbances, dermal and ocular irritation, nasal congestion, nausea, and diarrhea.<sup>[5,6]</sup> Moreover, increasing evidence suggests that long-term or prenatal exposure to OP pesticides and their metabolites may contribute to neurological disorders, particularly in children, by elevating the risk of attention deficit hyperactivity disorder (ADHD).<sup>[7,8]</sup> Given these serious health and environmental concerns, the development of rapid, sensitive, accurate, and reliable analytical methods for the detection of OP pesticides is of great importance.<sup>[9]</sup>

<sup>1</sup>Center of Physical Chemical Methods of Research and Analysis, Al-Farabi Kazakh National University, 96a Tole bi Street, Almaty, 050012, Kazakhstan

<sup>2</sup>Abai Kazakh National Pedagogical University, 13 Dostyk avenue, Almaty, 050010, Kazakhstan

\*Email: [y.bakytkarim@abaiuniversity.edu.kz](mailto:y.bakytkarim@abaiuniversity.edu.kz) (Yrysgul Bakytkarim)

Conventional analytical techniques such as gas chromatography (GC), liquid chromatography (LC), and high-performance liquid chromatography (HPLC) are widely recognized as reliable and well-established approaches for the detection and quantification of organophosphorus pesticides (OPPs).<sup>[10]</sup> These techniques are highly sensitive and precise, enabling the accurate measurement of OPPs even in complex sample matrices. However, despite their robustness, their broader applicability is restricted by several inherent drawbacks. In particular, GC, LC, and HPLC require sophisticated, high-cost instrumentation, as well as specialized laboratory facilities and skilled personnel for operation.<sup>[11]</sup> Moreover, these techniques typically involve laborious, multi-step sample preparation procedures, which not only increase the time and cost of analysis but may also introduce errors or analyte loss during pretreatment. Consequently, although these techniques are invaluable in controlled laboratory environments, they are less suitable for routine, on-site, or large-scale monitoring of pesticide residues in food and environmental samples.

In recent years, nanomaterial-based electrochemical sensors have gained significant attention as promising alternatives to conventional detection methods, primarily due to their high sensitivity, low cost, and operational simplicity. Among these, acetylcholinesterase (AChE)-based biosensors have been extensively explored, as they combine the advantages of straightforward fabrication with excellent sensitivity and strong selectivity toward organophosphorus compounds.<sup>[12-14]</sup> The principle of detection is based on the irreversible inhibition of AChE by OPPs, leading to measurable changes in the enzyme's electrochemical signal. While this approach offers significant advantages, AChE-based biosensors are not without limitations. The intrinsic instability of biological enzymes often leads to poor long-term durability, reduced reproducibility, and limited reusability.<sup>[15]</sup> These shortcomings restrict their applicability in real-world scenarios, especially in field-based pesticide monitoring where sensor robustness is critical. As a result, increasing attention has shifted toward the development of non-enzymatic electrochemical sensors. These devices bypass the drawbacks associated with biological components and instead exploit the electrocatalytic properties of metals and metal oxides. Materials such as CuO, ZnO, Fe<sub>2</sub>O<sub>3</sub>, Co<sub>3</sub>O<sub>4</sub>, and NiO have been widely investigated owing to their low cost, excellent electrocatalytic activity, and ability to facilitate electrochemical reactions at relatively low potentials.<sup>[16-18]</sup> Among them, copper and its oxides are particularly noteworthy due to their strong affinity for sulfur-containing compounds, a property that has been exploited for selective pesticide detection.<sup>[19,20]</sup> For instance, Razium *et al.* reported the development of an electrochemical sensor employing triangular CuO nanosheets for the sensitive detection of malathion.<sup>[21]</sup> In this system, CuO electrodes displayed well-defined redox peaks in a blank buffer solution. However, upon the addition of malathion, these electrochemical signals were

markedly suppressed, which was attributed to strong interactions between CuO and the analyte. This inhibition effect enabled the indirect quantification of malathion by monitoring changes in the CuO redox response. While effective, this method is inherently limited by its poor selectivity, as it is primarily tailored for malathion detection and cannot be broadly applied to other organophosphorus pesticides.

To address the inherent shortcomings of existing methods, in this study we developed a novel multi-analyte electrochemical sensor platform designed for the impedimetric detection of a broader spectrum of organophosphorus pesticides (OPPs), with particular emphasis on dichlorvos (DDVP). Unlike conventional single-target sensors, the proposed system is engineered to accommodate the simultaneous detection of multiple analytes, thereby enhancing its applicability in real-world scenarios where complex pesticide mixtures are frequently encountered.<sup>[22,23]</sup> The sensor architecture is based on a glassy carbon electrode (GCE) functionalized with multi-walled carbon nanotubes (MWCNTs) and gold nanoparticles (AuNPs). This hybrid modification strategy was selected due to the synergistic properties of the two nanomaterials: MWCNTs provide a large electroactive surface area and outstanding conductivity,<sup>[24,25]</sup> while AuNPs introduce superior electron-transfer kinetics and strong affinity toward organophosphorus compounds.<sup>[26,27]</sup> The integration of these materials not only accelerates charge transfer processes but also enhances analyte adsorption, significantly boosting sensor performance compared to conventional electrode systems.<sup>[28]</sup> The detection mechanism relies on electrochemical impedance spectroscopy (EIS) as an indirect analytical technique. Specifically, the interaction of DDVP with the modified electrode surface leads to the suppression of interfacial charge transfer, resulting in measurable impedance changes.<sup>[29]</sup> This inhibition-based approach eliminates the need for enzymatic or labeling components, ensuring simplicity, cost-effectiveness, and operational stability.<sup>[30,31]</sup> The fabricated sensor exhibited outstanding analytical characteristics, achieving an impressively low detection limit of 18.8 nM, with a wide and linear dynamic response range from 0.36  $\mu$ M to 1.8  $\mu$ M ( $R^2 = 0.99$ ). These results highlight the capability of the platform to detect trace levels of pesticides with high accuracy. Moreover, the system demonstrated excellent selectivity against potential interfering substances, underlining its robustness for complex sample matrices. Beyond its superior sensitivity and selectivity, the developed sensor offers several additional advantages. It is label-free, avoiding the cost and complexity associated with external markers; it is scalable and reproducible, which is critical for mass production; and it is adaptable for portable sensing devices, making it suitable for on-site environmental and food safety monitoring. Taken together, these attributes establish the proposed platform as a highly promising candidate for next-generation analytical technologies aimed at

ensuring food security, safeguarding public health, and protecting the environment from the harmful effects of organophosphorus pesticide contamination.

## 2. Experimental section

### 2.1 Chemicals and reagents

Chemically pure reagents were used throughout the experiments. Multi-walled carbon nanotubes (MWCNTs) were purchased from Nanjing Xianfeng nanomaterials Technology Co., Ltd.  $\text{HAuCl}_4 \cdot 2\text{H}_2\text{O}$  were purchased from Nanjing Xianfeng nanomaterials Technology Co., Ltd. All other chemicals were of analytical grade and used without further purification. The buffer solution was prepared using  $5 \text{ mmol/dm}^3 \text{ K}_3[\text{Fe}(\text{CN})_6]/\text{K}_4[\text{Fe}(\text{CN})_6]$  in the presence of  $0.1 \text{ M KCl}$ , with a total volume of  $25 \text{ mL}$ . This redox couple solution is well-suited for studying the electrochemical redox behavior of pesticides. Additionally, a phosphate buffer solution (PBS) was prepared by mixing  $0.1 \text{ M NaH}_2\text{PO}_4$  and  $0.1 \text{ M H}_3\text{PO}_4$  in a 1:1 volume ratio. The pH of the solution was adjusted as needed using acetic acid, sodium acetate, or sodium hydroxide solutions. The oxygen was removed from the solution by purging it with high-purity nitrogen (or argon) gas for approximately 10–15 minutes prior to the measurements. This procedure was performed to eliminate dissolved oxygen, which could interfere with the electrochemical measurements and to ensure the accuracy of the results. All aqueous solutions were prepared using double-distilled water.

### 2.2 Instruments and method

The experimental studies were carried out using an EC-Lab (BioLogic SP-300) potentiostat-galvanostat system. Electrochemical measurements were controlled and recorded using the “EC-Lab” software. All experiments were performed in the rmostated three-electrode electrochemical cells. The glassy carbon electrode (GCE) was used as the working electrode, an Ag/AgCl electrode as the reference electrode, and a platinum wire as the counter electrode. The chemical behavior of DDVP on the electrode was characterized by cyclic voltammetry (CV) and electrochemical impedance spectroscopy (EIS). Cyclic voltammetry is an electrochemical method based on measuring the dependence of the current on the potential of a polarized electrode in the analyte solution. This technique enables the evaluation of the overall oxidation or reduction capacity of a compound and is commonly used to investigate the electrochemical behavior of various antioxidant compounds by determining their redox potential. And electrochemical impedance spectroscopy (EIS) is a powerful technique used to analyze the resistance and capacitance of an electrochemical system by applying a small amplitude alternating voltage over a range of frequencies. EIS provides reliable information about processes occurring at the electrode surface, including reaction kinetics, charge transfer, and membrane properties. Scanning electron microscopy (SEM) and transmission electron microscopy (TEM) analyses

were carried out to comprehensively investigate the surface morphology, structural features, and dispersion characteristics of the synthesized multi-walled carbon nanotubes (MWCNTs) and gold nanoparticles (AuNPs) on the electrode surface. The JEM-1400 Plus is a  $120 \text{ kV}$  Transmission Electron Microscope (TEM) used at Nazarbayev University. It is equipped with a high-resolution polepiece and an advanced operation system, allowing both experts and beginners to operate it with ease. The instrument provides high-resolution TEM imaging, making it particularly suitable for research in medical and biological fields. Its high-resolution objective lens enables clear observation of specimens across a wide magnification range.

### 2.3 Preparation of multi-walled carbon nanotubes (MWCNTs) and decoration with gold nanoparticles (AuNPs)

First,  $0.1 \text{ g}$  of multi-walled carbon nanotubes (MWCNTs) was dispersed in  $50 \text{ mL}$  of  $6 \text{ M}$  nitric acid ( $\text{HNO}_3$ ) and refluxed under stirring for 12 hours. This acid treatment was carried out to remove impurities and amorphous carbon, as well as to introduce carboxyl ( $-\text{COOH}$ ) functional groups onto the surface of the MWCNTs. The presence of  $-\text{COOH}$  groups improves surface activity, enhances the dispersion of MWCNTs in aqueous media, facilitates the attraction and immobilization of gold ions, and promotes efficient electron transfer. After 12 hours, the suspension was filtered and washed several times with double-distilled water to remove residual acid. The functionalized MWCNTs were then ultrasonicated in ethanol to achieve uniform dispersion. Subsequently, the treated MWCNTs were added to a solution containing  $100 \text{ mM H}_2\text{SO}_4$  and  $2 \text{ mM}$  chloroauric acid ( $\text{HAuCl}_4 \cdot 2\text{H}_2\text{O}$ ) for gold nanoparticle (AuNP) deposition.

### 2.4 Preparation of MWCNTs-AuNPs/GCE impedimetric electrochemical sensor

As shown in Fig. 1, the modification of the GCE surface with MWCNTs-AuNPs: The surface of the glassy carbon electrode (GCE) was mechanically polished using an aluminum oxide ( $\text{Al}_2\text{O}_3$ ) paste for 15 minutes. After polishing, the electrode was immersed in ethanol and subjected to ultrasonic treatment for 6 minutes. Subsequently, the GCE was immersed for 1 hour in a mixture of  $0.5 \text{ M}$  nitric acid ( $\text{HNO}_3$ ) and  $0.1 \text{ M}$  sulfuric acid ( $\text{H}_2\text{SO}_4$ ) in a 2:1 volume ratio, followed by thorough rinsing with double-distilled water. For the modification step, the cleaned GCE was immersed in a prepared solution containing functionalized MWCNTs and gold nanoparticle (AuNP) precursors for 5 hours. After rinsing with double-distilled water, the electrode was re-immersed in the same solution for an additional 3 hours. Finally, the modified MWCNTs-AuNPs/GCE electrode was rinsed with double-distilled water and dried in air.

## 3. Results and discussion

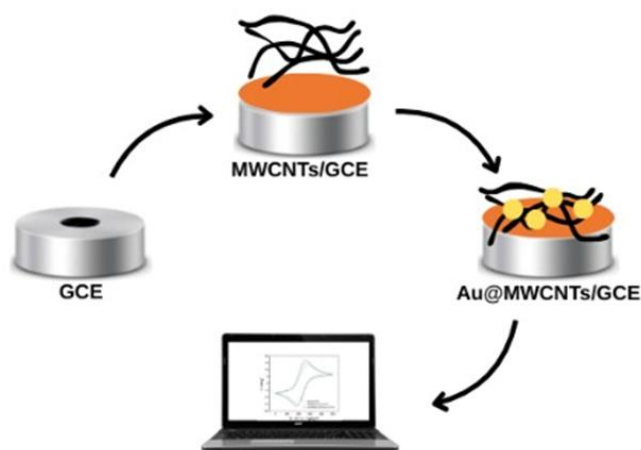


**Fig. 1:** Schematic representation of the surface modification of the glassy carbon electrode (GCE) with multi-walled carbon nanotubes (MWCNTs) decorated with gold nanoparticles (AuNPs).

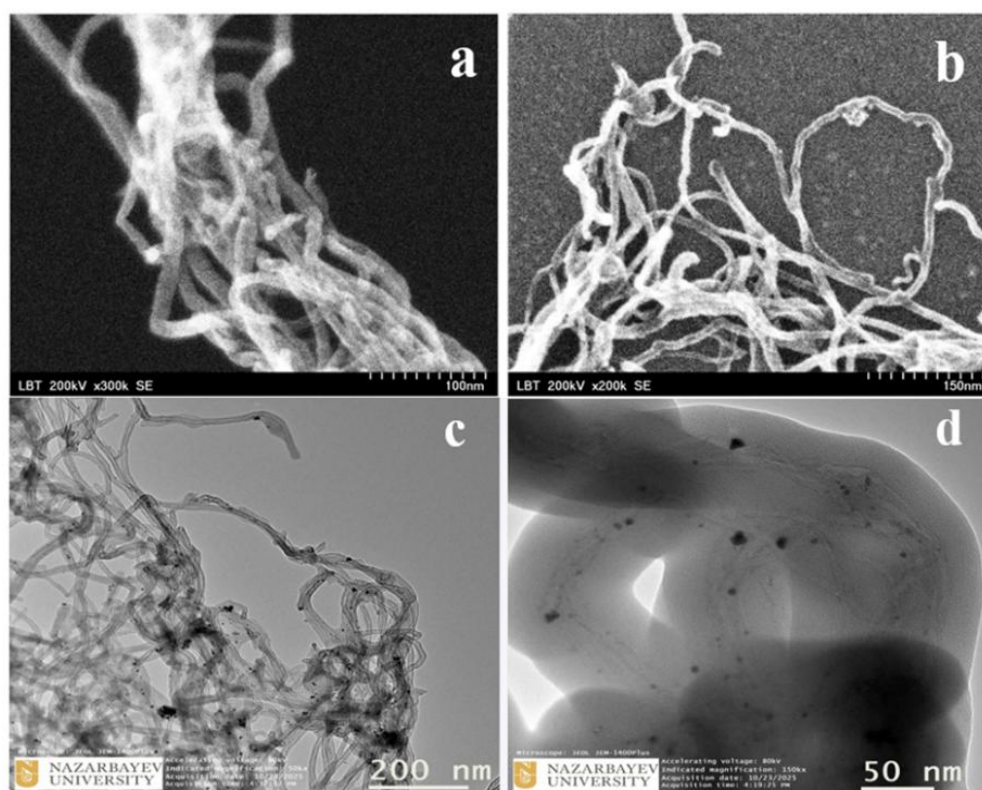


**Fig 2:** SEM images of (a) multi-walled carbon nanotubes (MWCNTs), (b) MWCNTs decorated with gold nanoparticles (MWCNTs-AuNPs) and TEM images of (c,d)MWCNTs decorated with gold nanoparticles (MWCNTs-AuNPs)

### 3.1 Morphology and characterization of nanocomposites

Scanning electron microscopy (SEM) and transmission electron microscopy (TEM) analyses were carried out to comprehensively investigate the surface morphology, structural features, and dispersion characteristics of the synthesized multi-walled carbon nanotubes (MWCNTs) and gold nanoparticles (AuNPs) on the electrode surface. In Fig. 2(a), the characteristic tubular network structure of MWCNTs is clearly observed, confirming their successful immobilization onto the glassy carbon electrode (GCE) surface. The nanotubes are uniformly dispersed, forming an interconnected fibrous structure that provides a large specific

surface area. This, in turn, creates favorable conditions for the subsequent attachment of nanoparticles and enhances the electrochemical activity of the electrode. Fig. 2(b) illustrates the distribution of gold nanoparticles (AuNPs) within the MWCNT framework. The AuNPs are densely and uniformly anchored along the nanotube surfaces with minimal aggregation, indicating strong interactions between the AuNPs and the functionalized sites of MWCNTs. Such a uniform coating improves the electrical conductivity and catalytic properties of the nanocomposite by providing a greater number of active sites for electron transfer processes. The nanoscale morphological features observed by SEM confirm

the successful formation of a stable and homogeneous MWCNT–AuNP composite layer on the electrode surface. Furthermore, to confirm the proper attachment of AuNPs on the MWCNTs, transmission electron microscopy (TEM) analysis was conducted. As shown in Fig. 2(c, d), the TEM images reveal that the gold nanoparticles (AuNPs) are well attached and uniformly distributed on the surface of the multi-walled carbon nanotubes (MWCNTs), demonstrating the successful preparation of the MWCNTs/AuNPs nanocomposite. In addition, to verify the elemental composition of the prepared nanocomposite, energy-dispersive X-ray spectroscopy (EDS) analysis was performed, and the results are presented in Fig. 3. The EDS spectrum confirms the presence of two predominant elements—carbon (C) and gold (Au)—corresponding to the MWCNTs and AuNPs, respectively. Quantitative analysis revealed that the relative weight percentages of carbon and gold were approximately 85.4 wt% and 14.6 wt%. The appearance of copper (Cu) peaks in the spectrum is attributed to the copper substrate used during SEM sample preparation and does not belong to the composite itself. Collectively, the SEM, EDS, and TEM analyses provide clear evidence that AuNPs were successfully integrated into the MWCNT matrix, resulting in a uniformly distributed nanocomposite with high structural stability and desirable physicochemical properties. Such morphology and composition are expected to significantly enhance the electrochemical performance of the modified electrode, particularly in applications requiring high

sensitivity and selectivity.

### 3.2 Electrochemical characterization of different modified electrodes

Cyclic voltammetry (CV) and electrochemical impedance spectroscopy (EIS) were employed to investigate the electrochemical properties of the AuNPs-MWCNTs-modified glassy carbon electrode (GCE). Fig. 4A presents the CV curves of the bare GCE (black), MWCNTs/GCE (red), and AuNPs-MWCNTs/GCE (blue) recorded in a 5 mmol/dm<sup>3</sup> K<sub>3</sub>[Fe(CN)<sub>6</sub>]/K<sub>4</sub>[Fe(CN)<sub>6</sub>] solution containing 0.1M KCl at a scan rate of 5 mV/s. For the bare GCE (black), a pair of reversible redox peaks is observed at approximately +260 mV (anodic) and +170 mV (cathodic). Upon modification with MWCNTs (red), a significant increase in both anodic and cathodic peak currents is observed due to the large effective surface area of the MWCNTs. Further modification with the AuNPs-MWCNTs nanocomposite (blue) leads to an even greater increase in redox peak currents and an elevated background current. This enhancement is attributed to the excellent electrical conductivity and enlarged electroactive surface area provided by the AuNPs-MWCNTs composite, which facilitates faster electron transfer at the electrode interface. Fig. 4B displays the corresponding Nyquist plots obtained from EIS measurements. The bare GCE (curve a) exhibits relatively high charge transfer resistance, while both the MWCNTs/GCE and AuNPs-MWCNTs/GCE (curve b) show significantly decreased resistance, indicating enhanced



Fig 3: The EDS results of MWCNTs-AuNPs nanocomposites.

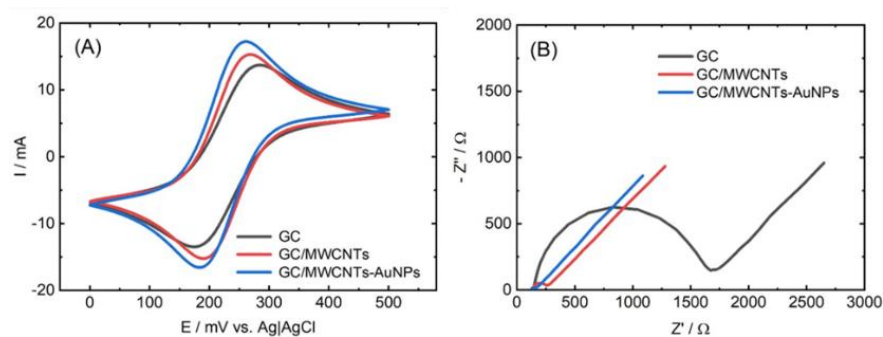


Fig 4: (A) CVs and (B) EIS of the bare GCE (black), MWCNTs/GCE (red), and AuNPs@MWCNTs/GCE (blue) recorded in a 5 mmol/dm<sup>3</sup> K<sub>3</sub>[Fe(CN)<sub>6</sub>]/K<sub>4</sub>[Fe(CN)<sub>6</sub>] solution containing 0.1M KCl at a scan rate of 5 mV/s.

charge transfer kinetics. Together, the CV and EIS results confirm the successful fabrication of the AuNPs-MWCNTs-modified GCE and demonstrate its superior electrochemical performance, highlighting its potential for use in sensitive and efficient electrochemical sensing applications.

### 3.3 Electrochemical behavior of DDVP at the MWCNTs-AuNPs/GCE electrode Investigated by Cyclic Voltammetry

As shown in Fig. 5A, cyclic voltammetry (CV) (A) and differential pulse voltammetry (DPV) (B) were employed to investigate the electrochemical behavior of DDVP on the MWCNTs-AuNPs/GCE electrode. The experiments were conducted in 0.1 M phosphate-buffered saline (PBS, pH 6.5), which served as the supporting electrolyte. No electrochemical activity was observed in the PBS alone, indicating the absence of measurable faradaic currents. Upon the addition of 100  $\mu\text{M}$  DDVP, a distinct anodic oxidation peak appeared at approximately +270 mV, confirming that the oxidation of DDVP molecules occurs specifically at this potential. Furthermore, increasing the scan rate from 20 mV/s to 40 mV/s resulted in a proportional increase in the oxidation peak current, indicating that the oxidation process is diffusion-controlled and occurs at the electrode surface. However, the overall electrochemical response was relatively weak. In particular, the DPV results shown in Fig. 5B also exhibited a very low anodic oxidation peak current. This limited and unstable current response suggests that amperometric detection of DDVP using CV and DPV is not sufficiently sensitive for reliable analysis. Therefore, due to the poor sensitivity and instability of the voltammetric signals, these methods were not pursued for further analysis. Instead, electrochemical impedance spectroscopy (EIS) was employed as an alternative technique. EIS provides higher sensitivity and

reliability, particularly for detecting low-concentration analytes, by monitoring changes in interfacial charge transfer resistance. This technique allows for a more precise evaluation of electron transfer processes at the electrode surface, making it better suited for the indirect detection of DDVP in this study.

### 3.4 Analysis of electrochemical impedance spectroscopy (EIS) results

Electrochemical impedance spectroscopy (EIS) was used to evaluate the surface electrochemical properties of the electrode. Fig. 6A shows the Nyquist plot recorded for the unmodified bare glassy carbon electrode (GCE), which displays a clear semicircle. The diameter of this semicircle corresponds to the charge transfer resistance ( $R_{ct}$ ). Based on the shape and size of the curve, it can be concluded that the bare GCE exhibits relatively high charge transfer resistance, indicating sluggish interfacial electrochemical reactions and limited electron transfer at the electrode surface. Fig. 6B presents the Nyquist plots obtained after modifying the electrode with multi-walled carbon nanotubes (MWCNTs) and gold nanoparticles (AuNPs). A significant decrease in the semicircle diameter is observed, reflecting a drastic reduction in  $R_{ct}$  and a substantial acceleration of the electron transfer process. The nanomaterials' increased effective surface area and enhanced electrical conductivity are responsible for this improvement. MWCNTs, known for their excellent conductivity, facilitate rapid electron transport, while AuNPs serve as electrocatalytically active sites. The reduced  $R_{ct}$  values indicate a notable enhancement in the surface conductivity of the electrode and an overall improvement in electrochemical reaction efficiency. The synergistic effect between MWCNTs and AuNPs plays a key role in significantly enhancing the electrochemical performance of the modified electrode.

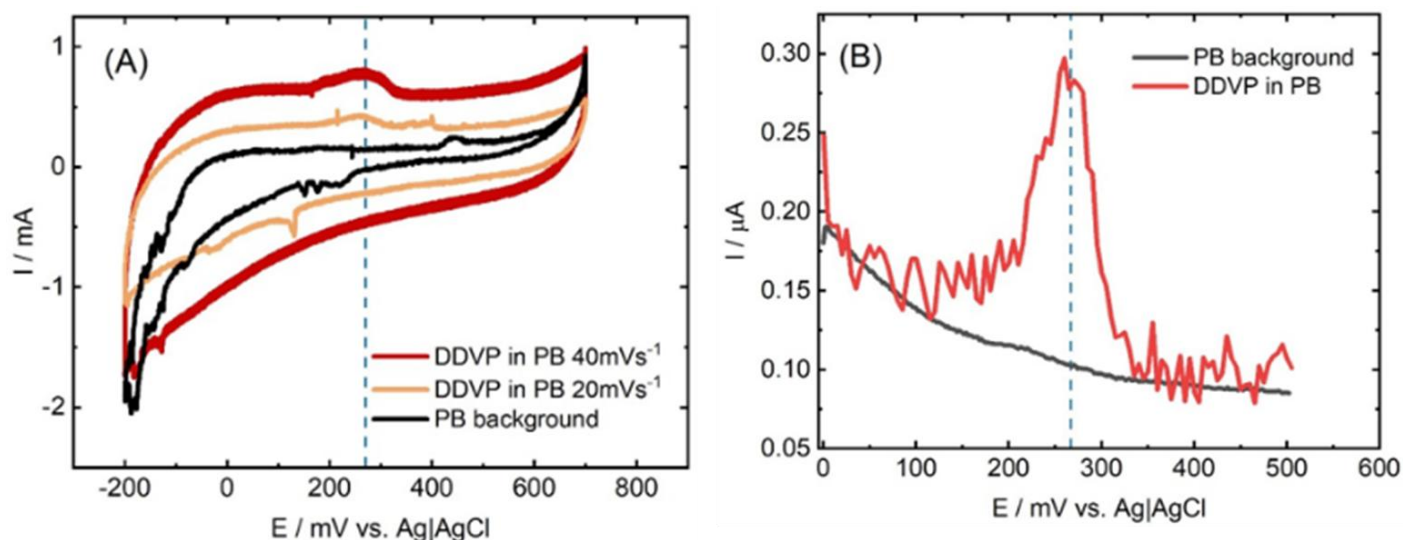


**Fig 5:** CV(A) and DPV(B) curves of the MWCNTs-AuNPs/GCE electrode recorded in 0.1M PBS solution pH 6.5 in presence of 100  $\mu\text{M}$  dichlorvos.

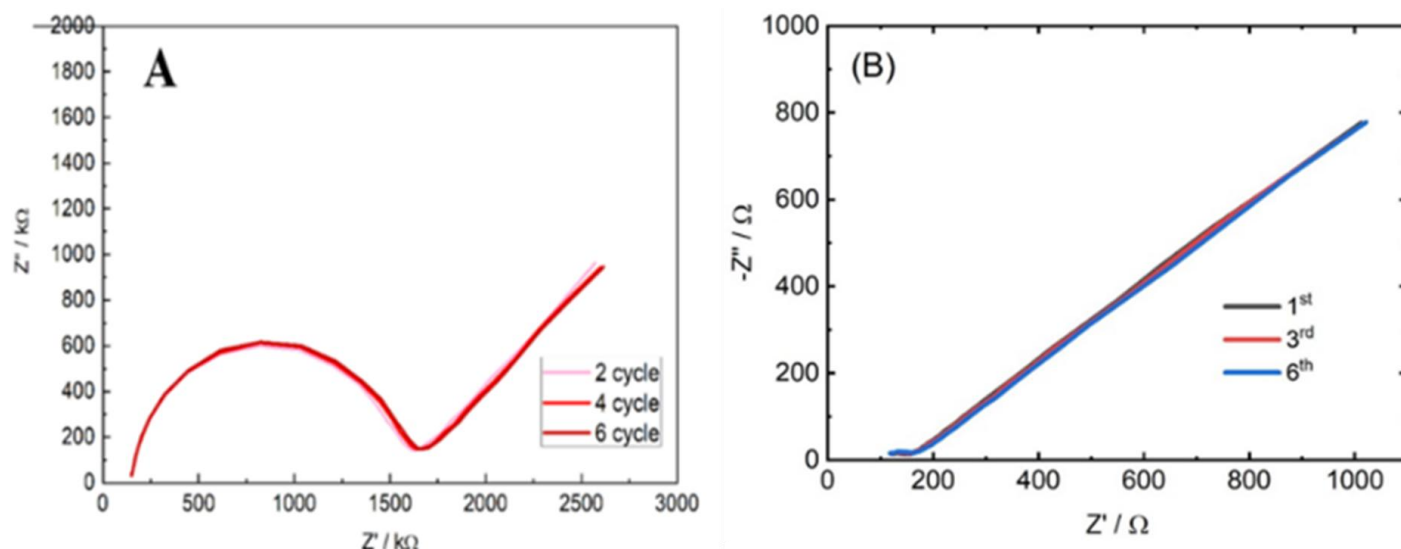


**Fig 6:** Nyquist plots of the bare GCE (A) and MWCNTs-AuNPs/GCE (B) electrode recorded over 6 cycles in a 5 mmol/dm<sup>3</sup> K<sub>3</sub>[Fe(CN)<sub>6</sub>]/K<sub>4</sub>[Fe(CN)<sub>6</sub>] solution containing 0.1M KCl.

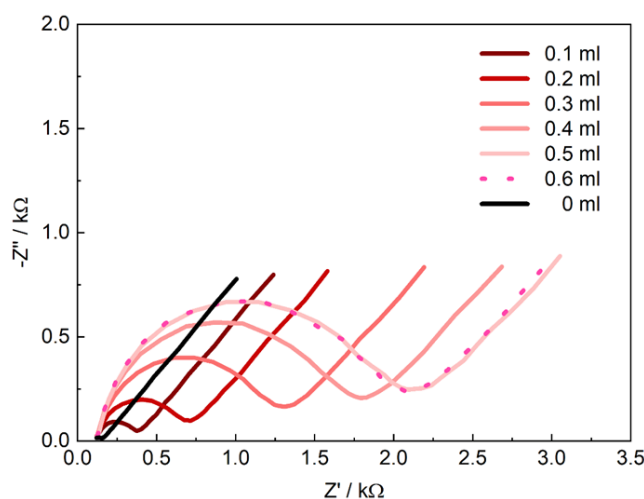


**Fig. 7:** Nyquist plots of the MWCNTs-AuNPs/GCE electrode recorded in 5 mM K<sub>3</sub>[Fe(CN)<sub>6</sub>]/K<sub>4</sub>[Fe(CN)<sub>6</sub>] + 0.1 M KCl solution with incremental additions of 0.1 to 0.6 mL of 45µM DDVP.

### 3.5 Quantitative determination of DDVP

As shown in Fig. 7 electrochemical impedance spectroscopy (EIS) was employed to investigate the interaction of the DDVP pesticide at the electrode surface. During the study, a solution of K<sub>3</sub>[Fe(CN)<sub>6</sub>]/K<sub>4</sub>[Fe(CN)<sub>6</sub>] with 0.1 M KCl was used as the redox probe. Various concentrations of 45µM DDVP pesticide (0.1 mL to 0.6 mL) were added to the solution, and the resulting Nyquist plots were used to evaluate the charge transfer characteristics of the system. The diameter of the semicircle in the Nyquist plot corresponds to the charge transfer resistance (R<sub>ct</sub>). As the concentration of DDVP increased, an enlargement in the semicircle diameter was observed, indicating that DDVP molecules adsorb onto the electrode surface and hinder the electron transfer process. The increase in pesticide concentration led to a decrease in the current signal and a corresponding increase in the charge transfer resistance, suggesting that DDVP participates in the oxidation process and slows down the electrochemical

reactions occurring at the electrode interface. As the concentration of DDVP increases, the corresponding rise in R<sub>ct</sub> values indicates diffusion-limited behavior, attributed to the formation of a barrier layer of pesticide molecules on the electrode surface. This layer hinders the access of redox species to electrode, resulting in a reduced rate of electron transfer. Such behavior is characteristic of analytes that strongly interact with the electrode surface and confirms the sensor’s sensitivity to the presence of DDVP. These findings further support the application of EIS as an effective technique for the indirect detection of organophosphorus pesticides through monitoring changes in interfacial charge transfer resistance.

Fig. 8 presents a calibration plot that illustrates the changes in charge transfer resistance (R<sub>ct</sub>) corresponding to various concentrations of DDVP pesticide. The obtained calibration line is described by the following Eq. (1):

$$R_{ct} = 1.318X - 0.0820 \tag{1}$$

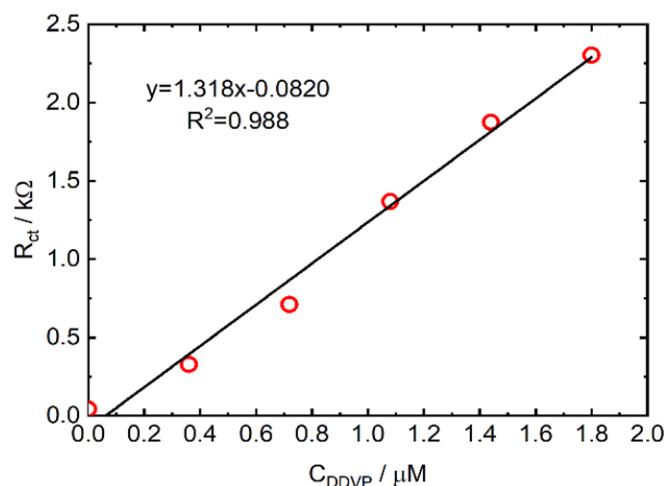


**Fig 8:** Calibration Curve for Impedimetric Detection of DDVP Pesticide on GCE/MWCNTs-AuNPs Electrode.

In this equation,  $R_{ct}$  represents the charge transfer resistance measured in ohms, while  $C$  denotes the concentration of DDVP expressed in  $\mu\text{mol/L}$ . The correlation coefficient value of  $R = 0.988$  confirms the high degree of linearity and demonstrates the analytical accuracy and reliability of the method. The sensitivity of the impedimetric method was evaluated through its limit of detection (LOD), which was calculated to be 18.8 nM. Moreover, compared with the most recently reported electrochemical sensors<sup>[32-35]</sup> for the determination of DDVP, our proposed nanocomposite sensor can perform ultrasensitive DDVP detection with a much wider linear range and significantly lower detection limits (Table 1). LOD was determined using the following Eq. (2):

$$\text{LOD} = \frac{3\sigma}{\text{slope}} \quad (2)$$

where:  $\sigma$  is the standard deviation of the signal, slope - is the slope of the calibration curve (1.318).

**Table 1:** Comparison of performances of the MWCNTs-AuNPs/GCE with other modified electrodes.

| Electrode  | Detection limit/(nM) | Linear range/(nM) | Ref       |
|--|----------------------|-------------------|-----------|
| Acetylcholinesterase/rGO @ Nafion /GCE                     | 9.05                 | 22.6-453          | [32]      |
| Acetylcholinesterase/chitosan @TiO <sub>2</sub> / rGO/ GCE | 29                   | 36-22600          | [33]      |
| ChOx/PBCBethaline-HNO <sub>3</sub> PTD                     | 1.6                  | 2.5-60            | [34]      |
| Nd <sub>2</sub> O <sub>3</sub> @MIL(Fe)-88A/GCE            | 0.92                 | 1-250             | [35]      |
| MWCNTs-AuNPs/GCE   | 18.8                 | 360-1800          | This work |

These results indicate that the sensor based on MWCNTs-AuNPs/GCE can detect extremely low concentrations of DDVP pesticide with high sensitivity and reliability. This

demonstrates its potential applicability for monitoring DDVP residues in environmental and food samples.

### 3.6 Selectivity, stability, and reproducibility of the Sensor

First, the effects of 0.5mM common inorganic ions and 50nM organic molecules on the detection of DDVP were examined. As shown in Fig. 9, the influence of various potential interferences on the Nyquist plot semicircle diameter was evaluated. For this purpose, 0.3 mL of 45  $\mu\text{M}$  DDVP was added to 15 mL of  $\text{K}_3[\text{Fe}(\text{CN})_6]/\text{K}_4[\text{Fe}(\text{CN})_6]$  solution containing 0.1 M KCl, which served as the redox probe. The presence of 0.5 mM inorganic ions had minimal effect on the semicircle diameter, indicating that these ions did not cause significant electrochemical interference. Similarly, the current variation in the presence of 50nM organic molecules was less than 2%, confirming the excellent selectivity of the MWCNTs-AuNPs/GCE sensor. These results suggest that DDVP molecules effectively adsorb onto the electrode surface and hinder electron transfer, thereby producing a measurable impedance signal.

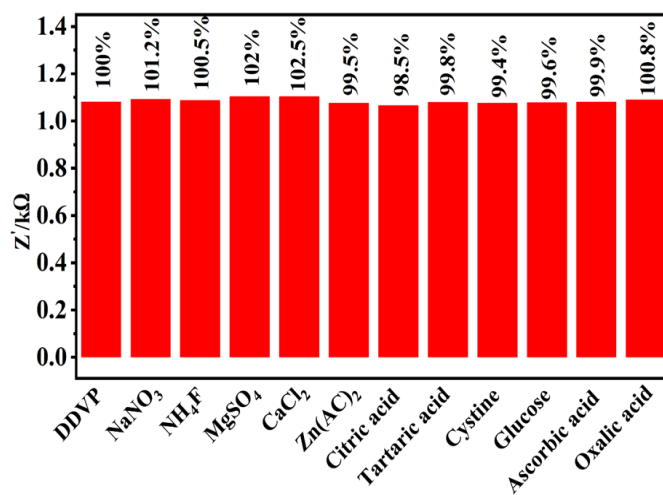


**Fig 9:** Effect of 0.5 mM inorganic ions and 50 nM organic molecules on the response signal of 0.9  $\mu\text{M}$  DDVP current at MWCNTs-AuNPs/GCE. (A 0.3 mL aliquot of 45  $\mu\text{M}$  DDVP was added to 15 mL of  $\text{K}_3[\text{Fe}(\text{CN})_6]/\text{K}_4[\text{Fe}(\text{CN})_6]$  solution containing 0.1 M KCl.)

### 3.7 Detection of DDVP in real samples

To evaluate the practical utility of the proposed sensor, the standard addition method was applied for the determination of DDVP in real water samples. As shown in Table 2, the recoveries were within the range of 97.2–101.9%, while the relative standard deviation (RSD) values for three replicate measurements were below 0.57%. These results indicate excellent accuracy, precision, and reproducibility, suggesting that potential matrix effects from real samples did not significantly interfere with the detection process. The obtained recovery rates confirm that the sensor is capable of accurate quantification of DDVP at trace levels in complex water matrices. Taken together, these findings highlight the strong

**Table 2:** Determination of DDVP in Actual Water Samples (n=3).

| Sample | Added ( $\mu\text{M}$ ) | Found ( $\mu\text{M}$ ) | Recovery (%) | RDS (%) |
|--------|-------------------------|-------------------------|--------------|---------|
| 1      | 0.9                     | 0.8848                  | 98.32        | 0.57    |
| 2      | 1.5                     | 1.4580                  | 97.2         | 0.18    |
| 3      | 1.7                     | 1.7323                  | 101.9        | 0.28    |

applicability of the developed sensing platform for practical environmental monitoring and routine pesticide residue analysis.

#### 4. Conclusion

In conclusion, a novel impedimetric electrochemical sensor based on a glassy carbon electrode modified with multi-walled carbon nanotubes (MWCNTs) and gold nanoparticles (AuNPs) has been successfully developed for the indirect detection of dichlorvos (DDVP). The synergistic effect of MWCNTs and AuNPs significantly enhanced the electroactive surface area, conductivity, and interfacial electron transfer properties of the electrode, thereby enabling highly sensitive and selective pesticide detection. The fabricated sensor demonstrated excellent analytical performance, with a low detection limit of 18.8 nM and a broad linear range of 0.36  $\mu\text{M}$  to 1.8  $\mu\text{M}$  ( $R^2 = 0.99$ ). The proposed impedimetric strategy, which relies on the inhibition of charge transfer by DDVP at the electrode–electrolyte interface, provides a label-free, cost-effective, and facile detection platform. Moreover, the robustness, reproducibility, and simplicity of this sensor make it a promising candidate for integration into portable and miniaturized devices, addressing the increasing demand for real-time pesticide monitoring. Considering the global concern over pesticide contamination and its severe implications for ecosystems and public health, the developed sensor provides not only an efficient analytical tool but also contributes toward sustainable agricultural practices and environmental protection. Future work may focus on extending this approach to the detection of other organophosphorus pesticides and exploring its performance in complex real-world matrices, thereby further advancing its practical utility.

#### Acknowledgments

This study was funded by the Scientific Committee of the Ministry of Science and Higher Education of the Republic of Kazakhstan (AP19676917 "Preparation of sensors by electrochemical methods for the determination of pesticides").

#### Conflict of Interest

There is no conflict of interest.

#### Supporting Information

Not applicable.

#### CRedit Statement

**Yrysgul Bakytkarim:** Supervision, Project administration, Funding acquisition. **Dilyara Yenbekova** and **Gulmira**

**Rakhymbay:** Experimental work, Methodology, Data curation. **Yerbol Tileuberdi** and **Yrysgul Bakytkarim:** Resources, Data curation, Writing – Review & editing. **Khaisa Avchukir:** Investigation, Writing – Original draft, Experimental work. **Nurgul Shadin** and **Zhazira Mukatayeva:** Formal analysis, Resources, Data collection.

#### References

- [1] M. Jokanović, Biotransformation of organophosphorus compounds, *Toxicology*, 2001, **166**, 139-160, doi: 10.1016/s0300-483x(01)00463-2.
- [2] L. G. Costa, Current issues in organophosphate toxicology, *Clinica Chimica Acta*, 2006, **366**, 1-13, doi: 10.1016/j.cca.2005.10.008.
- [3] M. Eddleston, L. Karalliedde, N. Buckley, R. Fernando, G. Hutchinson, G. Isbister, F. Konradsen, D. Murray, J. C. Piola, N. Senanayake, R. Sheriff, S. Singh, S. B. Siwach, L. Smit, Pesticide poisoning in the developing world: a minimum pesticides list, *The Lancet*, 2002, **360**, 1163-1167, doi: 10.1016/s0140-6736(02)11204-9.
- [4] M. Lotti, Clinical toxicology of anticholinesterase agents in humans, *Handbook of Pesticide Toxicology*, 2001, 1043-1085, doi: 10.1016/b978-012426260-7/50054-9.
- [5] M. B. Abou-Donia, Organophosphorus ester-induced chronic neurotoxicity, *Archives of Environmental Health*, 2003, **58**, 484-497, doi: 10.3200/aeoh.58.8.484-497.
- [6] H.-W. Chang, C.-L. Chen, Y.-H. Chen, Y.-M. Chang, F.-J. Liu, Y.-C. Tsai, Electrochemical organophosphorus pesticide detection using nanostructured gold-modified electrodes, *Sensors*, 2022, **22**, 9938, doi: 10.3390/s22249938.
- [7] M. F. Bouchard, D. C. Bellinger, R. O. Wright, M. G. Weisskopf, Attention-deficit/hyperactivity disorder and urinary metabolites of organophosphate pesticides, *Pediatrics*, 2010, **125**, e1270-e1277, doi: 10.1542/peds.2009-3058.
- [8] V. Rauh, S. Arunajadai, M. Horton, F. Perera, L. Hoepner, D. B. Barr, R. Whyatt, Seven-year neurodevelopmental scores and prenatal exposure to chlorpyrifos, a common agricultural pesticide, *Environmental Health Perspectives*, 2011, **119**, 1196-1201, doi: 10.1289/ehp.1003160.
- [9] Y. Li, H. Zhang, P. Wu, L. Cui, Recent advances in nanomaterial-based electrochemical sensors for organophosphorus pesticide detection, *Biosensors and Bioelectronics*, 2023, **231**, 115291, doi: 10.1016/j.bios.2023.115291.
- [10] Z. Zhang, J. Liu, J. Wang, Gas chromatography and liquid chromatography techniques for pesticide residue analysis: A critical review, *Journal of Chromatography A*, 2022, **1672**, 463075, doi: 10.1016/j.chroma.2022.463075.
- [11] Z. Huang, D. Sun, Z. Xu, Challenges and advances in sample preparation for pesticide residue analysis: Towards greener and simpler approaches, *TrAC Trends in Analytical Chemistry*, 2024, **169**, 117070, doi: 10.1016/j.trac.2023.117070.
- [12] F. Li, Y. Liu, Y. Zhang, Recent progress in AChE-based biosensors for pesticide detection: A review, *Biosensors and Bioelectronics*, 2023, **231**, 115280, doi:

- 10.1016/j.bios.2023.115280.
- [13] J. Wang, Q. He, M. Zhou, Advances in acetylcholinesterase biosensors for organophosphorus pesticide detection, *Microchimica Acta*, 2024, **191**(3), 120, doi: 10.1007/s00604-024-05837-y.
- [14] R. Sharma, A. Singh, AChE-based electrochemical biosensors: Challenges and future perspectives, *TrAC Trends in Analytical Chemistry*, 2022, **149**, 116546, doi: 10.1016/j.trac.2022.116546.
- [15] X. Chen, J. Gao, P. Wu, Improving the stability of AChE biosensors: Recent strategies and materials, *Sensors and Actuators B: Chemical*, 2023, **377**, 133019, doi: 10.1016/j.snb.2023.133019.
- [16] Y. Huang, J. Liu, X. Ma, Non-enzymatic electrochemical sensors for pesticide detection based on metal and metal oxide nanomaterials, *Electrochimica Acta*, 2024, **478**, 142030, doi: 10.1016/j.electacta.2023.142030.
- [17] K. Zhang, J. Li, D. Sun, Metal oxide nanostructures for non-enzymatic sensing of organophosphorus pesticides, *Analytica Chimica Acta*, 2022, **1203**, 339703, doi: 10.1016/j.aca.2022.339703.
- [18] L. Zhao, H. Wang, M. Qiao, Recent development of transition metal oxide-based electrochemical sensors for environmental monitoring, *Journal of Hazardous Materials*, 2023, **447**, 130895, doi: 10.1016/j.jhazmat.2023.130895.
- [19] T. Wang, H. Zhao, Z. Chen, Recent advances in copper-based nanomaterials for sensing applications: Focus on sulfur-containing species, *Sensors and Actuators B: Chemical*, 2023, **380**, 133321, doi: 10.1016/j.snb.2023.133321.
- [20] Y. Zhang, H. Liu, W. Sun, Affinity of copper oxide nanostructures toward thiol-containing analytes: Mechanistic insights and sensor applications, *Electrochimica Acta*, 2022, **418**, 140343, doi: 10.1016/j.electacta.2022.140343.
- [21] A. Raziq, M. Ali, M. Khan, Sensitive detection of malathion using a triangular CuO nanosheet-modified electrode: A study based on redox inhibition mechanism, *Microchimica Acta*, 2024, **191**(5), 211, doi: 10.1007/s00604-024-06002-1.
- [22] J. Ping, J. Wu, Y. Wang, Y. Ying, Development of an electrochemical biosensor for pesticide detection, *Biosensors and Bioelectronics*, 2012, **28**(1), 35–42, doi: 10.1016/j.bios.2011.06.046.
- [23] J. Wang, Electrochemical biosensors: Towards point-of-care cancer diagnostics, *Biosensors and Bioelectronics*, 2006, **21**, 1887-1892, doi: 10.1016/j.bios.2005.10.027.
- [24] H. Teymourian, M. Parrilla, J. R. Sempionatto, N. F. Montiel, A. Barfidokht, R. Van Echelpoel, K. De Wael, J. Wang, Wearable electrochemical sensors for the monitoring and screening of drugs, *ACS Sensors*, 2020, **5**, 2679-2700, doi: 10.1021/acssensors.0c01318.
- [25] S. Liu, H. Ju, Electrochemical biosensors based on functional nanomaterials, *Biosensors and Bioelectronics*, 2003, **19**(2), 177–184, doi: 10.1016/S0956-5663(03)00161-5.
- [26] M.-C. Daniel, D. Astruc, Gold nanoparticles: assembly, supramolecular chemistry, quantum-size-related properties, and applications toward biology, catalysis, and nanotechnology, *Chemical Reviews*, 2004, **104**, 293-346, doi: 10.1021/cr030698+.
- [27] G. Doria, J. Conde, B. Veigas, L. Giestas, C. Almeida, M. Assunção, J. Rosa, P. V. Baptista, Noble metal nanoparticles for biosensing applications, *Sensors*, 2012, **12**, 1657-1687, doi: 10.3390/s120201657.
- [28] A.A. Ensafi, B. Rezaei, Electrochemical sensors and biosensors based on metal oxide nanoparticles, *TrAC Trends in Analytical Chemistry*, 2019, **118**, 182–193, doi: 10.1016/j.trac.2019.05.038.
- [29] E. Katz, I. Willner, Probing biomolecular interactions at conductive and semiconductive surfaces by impedance spectroscopy: routes to impedimetric immunosensors, DNA-sensors, and enzyme biosensors, *Electroanalysis*, 2003, **15**, 913-947, doi: 10.1002/elan.200390114.
- [30] W. Putzbach, N. Ronkainen, Immobilization techniques in the fabrication of nanomaterial-based electrochemical biosensors: a review, *Sensors*, 2013, **13**, 4811-4840, doi: 10.3390/s130404811.
- [31] F. Arduini, S. Cinti, V. Scognamiglio, D. Moscone, G. Palleschi, How cutting-edge technologies impact the design of electrochemical (bio)sensors for environmental analysis. A review, *Analytica Chimica Acta*, 2017, **959**, 15-42, doi: 10.1016/j.aca.2016.12.035.
- [32] S. Wu, F. Huang, X. Lan, X. Wang, J. Wang, C. Meng, Electrochemically reduced graphene oxide and Nafion nanocomposite for ultralow potential detection of organophosphate pesticide, *Sensors and Actuators B: Chemical*, 2013, **177**, 724-729, doi: 10.1016/j.snb.2012.11.069.
- [33] H.-F. Cui, W.-W. Wu, M.-M. Li, X. Song, Y. Lv, T.-T. Zhang, A highly stable acetylcholinesterase biosensor based on chitosan-TiO<sub>2</sub>-graphene nanocomposites for detection of organophosphate pesticides, *Biosensors and Bioelectronics*, 2018, **99**, 223-229, doi: 10.1016/j.bios.2017.07.068.
- [34] O. Tutunaru, C. M. Mihailescu, M. Savin, B. C. Tincu, M. C. Stoian, G. S. Muscalu, B. Firtat, S. Dinulescu, G. Craciun, C. A. Moldovan, A. Fica, A. C. Ion, Acetylcholinesterase entrapment onto carboxyl-modified single-walled carbon nanotubes and poly (3, 4-ethylenedioxythiophene) nanocomposite, film electrosynthesis characterization, and sensor application for dichlorvos detection in apple juice, *Microchemical Journal*, 2021, **169**, 106573, doi: 10.1016/j.microc.2021.106573.
- [35] M. Narayanan, N. P. Singh Chauhan, P. Perumal, A highly efficient metal oxide incorporated metal organic framework [Nd<sub>2</sub>O<sub>3</sub>-MIL(Fe)-88A] for the electrochemical detection of dichlorvos, *RSC Advances*, 2023, **13**, 5565-5575, doi: 10.1039/d2ra07877e.

**Publisher's Note:** Engineered Science Publisher remains neutral with regard to jurisdictional claims in published maps and institutional affiliations.

### Open Access

This article is licensed under a Creative Commons Attribution 4.0 International License, which permits the use, sharing, adaptation, distribution and reproduction in any medium or

format, as long as appropriate credit to the original author(s) and the source is given by providing a link to the Creative Commons license and changes need to be indicated if there are any. The images or other third-party material in this article are included in the article's Creative Commons license, unless indicated otherwise in a credit line to the material. If material is not included in the article's Creative Commons license and your intended use is not permitted by statutory regulation or exceeds the permitted use, you will need to obtain permission directly from the copyright holder. To view a copy of this license, visit <http://creativecommons.org/licenses/by/4.0/>.

©The Author(s) 2025.